Songklanakarin J. Sci. Technol.
42 (3), 705-713, May - Jun. 2020

http://www.sjst.psu.ac.th

*Original Article*

# Optimization of surface roughness and microhardness using the Taguchi method in conventional and ultrasonic-assisted milling of aluminum A356

Sed Udomboonyanupap[1], Somsak Siwadamrongpong[1*], Apiwat Muttamara[2], and Thongchai Pangjundee[3]

[1] *School of Manufacturing Engineering, Suranaree University of Technology, Mueang, Nakhon Ratchasima, 30000 Thailand*

[2] *Department of Industrial Engineering, Faculty of Engineering, Thammasat University, Ransit Campus, Khlong Luang, Pathum Thani, 12120 Thailand*

[3] *Faculty of Science and Technology, Bansomdejchaopraya Rajabhat University, Thon Buri, Bangkok, 10600 Thailand*

Received: 29 May 2018; Revised: 27 March 2019; Accepted: 31 March 2019

## Abstract

The Taguchi method and regression analysis were used to evaluate the machinability of aluminum A356 with conventional and ultrasonic-assisted milling. Experiments were carried out based on an orthogonal array $L_{18}$ with three parameters (milling condition, spindle speed, and feed rate). According to the signal to noise ratio (S/N), the optimal surface roughness condition was determined at A1B3C1 (i.e., milling condition was conventional milling, spindle speed was 7000 rpm, and feed rate was 50 m/min). The optimal surface hardness condition was found at A2B1C3 (i.e., milling condition was ultrasonic-assisted milling, spindle speed was 3000 rpm, and feed rate was 400 m/min). Analysis of variance (ANOVA) was used to determine the effects of the machining parameters which showed that the feed rate was the main factor affecting surface roughness and microhardness. Linear and quadratic regression analyses were applied to predict the outcomes of the experiment. The predicted and measured values of surface hardness were close to each other while a large error was observed for the surface roughness prediction. Confirmation test results showed that the Taguchi method was successful in optimizing the machining parameters for minimum surface roughness and maximum microhardness in the milling of aluminum A365.

**Keywords:** ultrasonic-assisted milling, surface roughness, microhardness, Taguchi method, analysis of variance

## 1. Introduction

Surface integrity (SI) is one of the most relevant parameters used to evaluate the machined surface of a product. It represents the performance of material inner surfaces, such as surface topography, surface roughness, surface residual stress, and surface microhardness. Its quality importantly affects the wear rate, fatigue strength, and corrosion resistance of the components (Javidi, Rieger, & Eichlseder, 2008).

The milling process is the most commonly used method to remove material in the automotive and aircraft industries. The cutting parameters of the milling process, such as cutting speed, feed rate, and depth of cut, greatly influence the SI (Umbrello, 2013; Jin & Liu, 2011; Sun & Guo, 2009). Several researchers have studied and statistically optimized the cutting parameters to improve the SI. Rafai, Lajis, and Hosni (2014) studied the effect of the machining parameters

*Corresponding author
Email address: somsaksi@sut.ac.th

on SI of AISI D2. The results indicated that a higher cutting speed adversely affected the microhardness value of the subsurface layer. Daymi, Boujelbene, Amara, Bayraktar, and Katundi (2011) reported that the recorded high surface hardness values were due to a larger contact area between the cutting tool and the workpiece material. The top layer of a titanium alloy machined surface experienced work hardening and, therefore, the hardness values were higher than the hardness of the workpiece material. Shunyao, Minghe, Lansheng, Zhishou, and Xinnan (2016) optimized the surface integrity of ultra-high-strength titanium alloy by the Taguchi-Grey relational analysis method. The results reported that the preferred combination of process parameters was: milling speed of 100 m/min, a feed per tooth of 0.02 mm/tooth, a radial depth of cut of 1.5 mm, a rake angle of 18 degrees, and helix angle of 60°. Xiangyu *et al.* (2018) investigated the effects of cutting and feed rate on the surface integrity of Inconel 718 and found that although the cutting speed barely affected the surface roughness, the surface hardness increased as the cutting speed and feed rate increased. Erkan, Demetgul, Isik, and Tansel (2014) carried out the Taguchi method to evaluate the machinability of composite materials. The result of a ANOVA analysis was used to show that the cutting speed was the most significant factor affecting surface roughness.

In addition to SI improvement by cutting parameter optimization on conventional milling (CM), a recent and efficient technique to improve milling performance is known as ultrasonic-assisted milling (UAM). The fundamental feature of UAM is the tool face is separated from the chip and cutting area repeatedly by using high-frequency peak-to-peak vibration amplitude imposed on the tool or workpiece (Azarhoushang & Akbari, 2007; Chern & Chang, 2006). In the past few decades, different researchers have reported significant improvements in hard-brittle materials using UAM. Noma, Takeda, Aoyama, Kakinuma, and Hamada (2014) presented a reduction of thrust force, tool wear, and chipping size after applying axial ultrasonic vibration-assisted milling of chemically strengthened glass. Suarez *et al.* (2016) investigated the effect of ultrasonic vibration-assisted milling on difficult to cut Ni-Alloy 718. The results showed that ultrasonic milling resulted in increased fatigue which was possibly due to surface differences from conventional milling. Elhami, Razfar, and Farahnakian (2015) could reduce the cutting force of hardened AISI 4140 machining process by applying two advanced machining methods: thermally enhanced machining and UAM to the workpiece. Uhlmann, Protz, Stawiszyndski, and Heidler (2017) studied the effects of UAM when a different cutting condition was applied to carbon and glass fiber reinforced plastics. The results showed that UAM can be advantageous on workpiece quality and dust concentration but a reduction of cutting force could not be observed. Razfar, Sarvi, and Zarchi (2011) investigated the effect of UAM of AISI 1020 steel in terms of depth of cut, cutting speed, and feed rate. The surface roughness improved by up to 12.9% when implementing UAM. Maurotto and Wickramarachchi (2016) investigated the effect on residual stresses in the UAM of AISI 316L reaching frequencies as high as 60 kHz, but they found the best results in the low-frequency range.

Overall, UAM is an advanced machining technology and has contributed several advantages. However, the literature review shows that almost no research work has been performed related to optimizing the ductile material surface integrity using the UAM technique. This research aimed to expand UAM research of SI into a wider variety of materials and applications. Therefore, this study presents the results of UAM cutting parameter effects on the SI of a ductile material, namely aluminum A356 alloy. This aluminum alloy is preferable because of attractive properties that include high strength-to-weight ratio, pressure tightness, excellence weld-ability, high corrosion resistance, and good casting and machining characteristics. Furthermore, aluminum A356 is widely used in the automobile and aircraft industries.

In this study, the effects of machining parameters were investigated on the surface roughness and microhardness in the milling of aluminum A356 with conventional milling and UAM. Taguchi's $L_{18}$ array was applied to conduct the experiments. Taguchi's signal-to-noise ratio was calculated to identify minimum surface roughness and maximum surface microhardness to determine the optimal machining conditions (i.e., milling condition, spindle speed, and feed rate). In addition, linear and quadratic regression analyses were used to predict the measured values. Finally, the developed models were tested by confirmation experiments.

## 2. Materials and Methods

### 2.1 Material

Aluminum A356 T6 was used for this experiment. The workpiece material was cut to the dimension of 10x50x20 mm. The elemental compositions of the workpiece material are shown in Table 1.

Table 1. Percentages of alloying elements used in aluminum A356 T6.

| Si | Mg | Fe | Cu | Mn | Zn | Ti | Al |
|---|---|---|---|---|---|---|---|
| 7.18 | 0.215 | 0.108 | 0.0197 | 0.0045 | 0.0089 | 0.112 | Bal. |

### 2.2 Ultrasonic-assisted milling (UAM) experiments

The experiments of the UAM process were performed on a 3-axis UMACH LMC1020 CNC milling machine. An ultrasonic generator (UCE Ultrasonic) was employed to supply high-frequency electrical impulses into a 1.5 kW piezoelectric transducer. These high-frequency electrical pulses are converted to mechanical vibrations at an ultrasonic frequency (19.74 kHz) and transferred to the aluminum A365 workpiece which is attached at the end of the transducer. An ultrasonic transducer body was fixed with a transducer holder clamped with a holder base by four hex head set screws. A bench vise on the CNC machine table was used to clamp the transducer holder base (Figure 1).

The vibration amplitude of the workpiece was measured by a Keyence EV-101V eddy current sensor. The sensor probe was located at a distance of 1 mm from the end face of the workpiece (Figure 2a). Vibration frequency signal was transferred through the eddy current sensor and Keyence controller EX-V02 to output at the Hantek DSO520P Digital oscilloscope monitor. The output voltage value was 84mV and its amplitude value was 12 µm peak to peak by voltage calculation (Figure 2b).

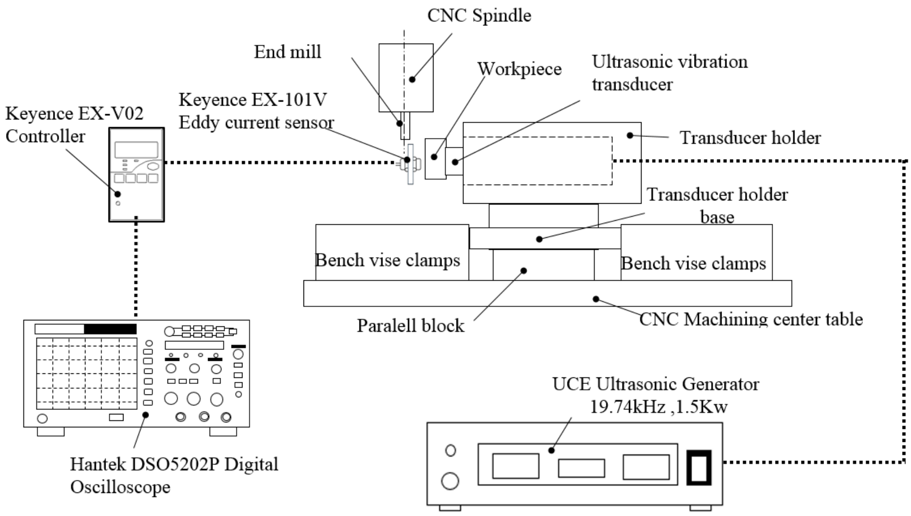


Figure 1. Schematic of experiment set up.

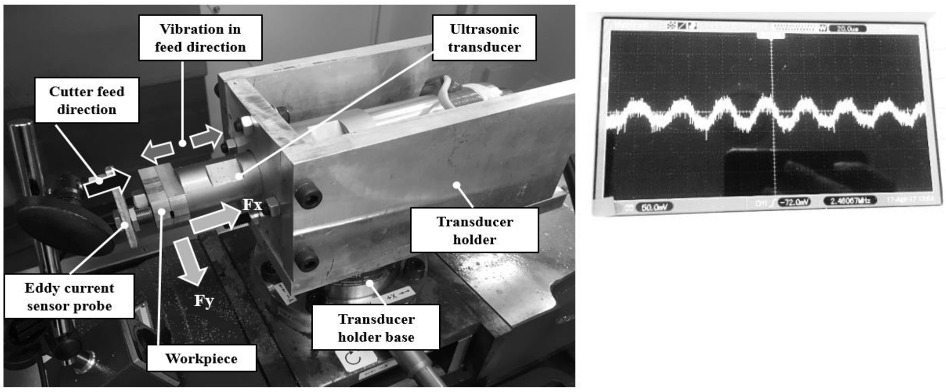


(a) (b)

Figure 2. (a) Set up of workpiece and sensor for vibration amplitude measurement and (b) output voltage from sensor measuring vibration amplitude (1 µm/7 mV) which shows the amplitude of 12 µm.

## 2.3 Surface roughness measurement

The average surface roughness (*Ra*) of the workpiece was measured by a Mitutoyo portable surface roughness tester model SJ-201. The surface roughness was measured parallel to the machined surface from three different points and the average values of the measurements were evaluated.

## 2.4 Microhardness measurement

Microhardness (*MH*) after machining was measured parallel to feed direction using a Vickers microhardness tester FM-800. The test load parameter was 100 gf with 10 sec of dwell time. Each measurement was repeated three times at different locations and the average value of each output was calculated.

## 2.5 Experiment design and optimization

The Taguchi method is widely used in the industry and is a highly efficient experiment design. It has been proven that this systematic approach can specify the optimum cutting parameters and improve the process performance (Kuram & Ozcelik, 2013; Sayuti, Sarhan, Fadzil, & Hamdi, 2012).

The Taguchi method uses a signal to represent the desirable value, and noise represents the undesirable value. The process parameter with the highest signal-to-noise (S/N) ratio (η) always yields the optimum quality with minimum variance (Phadke, 1989). There are three different functions of quality characteristics in the analysis of the S/N ratio, namely the lower-the-better, the higher-the-better, and the nominal-the-best (Gupta, Singh, & Aggarwal, 2011). For each level of the process parameters, the S/N ratio is calculated based on the objective function. The aim of this study was to minimize surface roughness and maximize microhardness. Therefore the lower-the-better and higher-the-better quality characteristics were used as shown in Equation 1 and Equation 2, respectively:

$$\eta = S/N_s = -10log\left[\frac{1}{n}\sum_{i=1}^{n} y_i^2\right] \quad (1)$$

$$\eta = S/N_s = -10log\left[\frac{1}{n}\sum_{i=1}^{n}\frac{1}{y_i^2}\right] \quad (2)$$

where $y_i$ is the observed data at the $i$th experiment and $n$ is the number of observations of the experiment (Mandal, Doloi, Mondal, & Das, 2011).

Milling conditions (*Mc*), spindle speed *(n*), and feed rate (*f*) were selected as the control factors. The levels of spindle speed and feed rate were determined based on the cutting tool manufacturer's recommended ranges. Their values are presented in Table 2. The mixed orthogonal array $L_{18}$ ($2^1$ x $3^2$) (Table 3) was used to conduct the experiments to determine the optimal cutting parameters and analyze the effects of the machining parameters.

Table 2. Milling parameters and levels.

| Parameter | Symbol | Level 1 | Level 2 | Level 3 |
|---|---|---|---|---|
| Milling conditions | A | CM | UAM | - |
| Spindle speed (rev/min) | B | 3000 | 5000 | 7000 |
| Feed rate (mm/min) | C | 50 | 200 | 400 |

Table 3. Full factorial design with orthogonal array of Taguchi $L_{18}$ ($2^1$ x $3^2$).

| Experiment no. | Factor A | Factor B | Factor C |
|---|---|---|---|
| 1 | 1 | 1 | 1 |
| 2 | 1 | 1 | 2 |
| 3 | 1 | 1 | 3 |
| 4 | 1 | 2 | 1 |
| 5 | 1 | 2 | 2 |
| 6 | 1 | 2 | 3 |
| 7 | 1 | 3 | 1 |
| 8 | 1 | 3 | 2 |
| 9 | 1 | 3 | 3 |
| 10 | 2 | 1 | 1 |
| 11 | 2 | 1 | 2 |
| 12 | 2 | 1 | 3 |
| 13 | 2 | 2 | 1 |
| 14 | 2 | 2 | 2 |
| 15 | 2 | 2 | 3 |
| 16 | 2 | 3 | 1 |
| 17 | 2 | 3 | 2 |
| 18 | 2 | 3 | 3 |

## 3. Results and Discussion

### 3.1. Analysis of the signal-to-noise (S/N) ratio

The *Ra* and *MH* were measured following the experimental design for each combination of the control factors using the Taguchi techniques. Table 4 shows the values of the S/N ratios of the surface roughness and micro-hardness. The average values of the surface roughness and microhardness were calculated to be 0.64 µm and 98.79 HV, respectively. In the same method, the average values of S/N ratio for surface roughness and microhardness were calculated to be 6.515 dB and 39.854 dB, respectively.

The effects of each control factor (*Mc*, *n*, *f*) on the surface roughness and microhardness were analyzed via the "S/N response table" (Table 5) which shows the optimal levels of control factors for the optimal surface roughness and microhardness values. The level values of control factors for *Ra* and *MH* in Table 5 are shown graphically in Figure 3. The highest S/N ratio in the levels of the control factors determined the best level for each control factor. Hence, the levels and S/N ratios for the factors giving the best *Ra* value were specified as factor A (Level 1, S/N = 6.591), factor B (Level 3, S/N = 10.434), and factor C (Level 1, S/N = 13.727). In other words, an optimum *Ra* value was obtained with a CM (A1), a spindle speed (B3) 7000 rev/min, and a feed rate (C1) 50 mm/min (Figure 3a). With the same method, the levels and S/N ratios for the factors giving the best *MH* were determined as factor A (Level 2, S/N = 40.34), factor B (Level 1, S/N = 40.44), and factor C (Level 3, S/N = 40.49). Therefore, the optimum *MH* value was obtained with a UAM (A2), a spindle speed of 3000 rev/min (B1), and a feed rate of 400 mm/min (C3) (Figure 3b).

Table 5. S/N response table for *Ra* and *MH* factors.

| Levels | Control factor | | | | | |
|---|---|---|---|---|---|---|
| | Surface roughness (*Ra*) | | | Microhardness (*MH*) | | |
| | A | B | C | A | B | C |
| Level 1 | 6.591 | 2.641 | 13.727 | 39.37 | 40.44 | 39.33 |
| Level 2 | 6.439 | 6.471 | 6.718 | 40.34 | 39.66 | 39.74 |
| Level 3 | - | 10.434 | -0.899 | - | 39.46 | 40.49 |
| Delta | 0.152 | 7.793 | 14.626 | 0.96 | 0.97 | 1.16 |

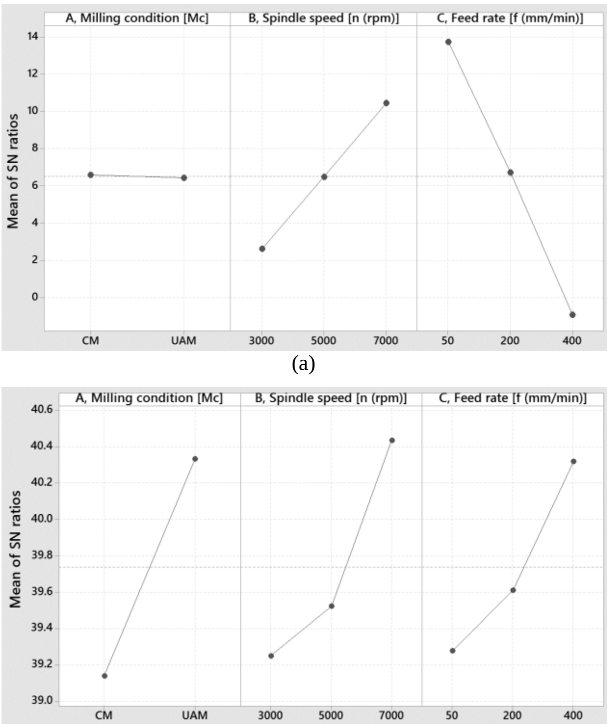


(a)

(b)

Figure 3. Effects of process parameters on (a) average S/N ratio for *Ra* and (b) average S/N ratio for *MH*.

Table 4. Results of the experiments and S/N ratio values.

| Experiment no. | Control factor | | | Surface roughness, *Ra* (μm) | S/N ratio for *Ra* (dB) | Microhardness, *MH* (HV) | S/N ratio for *MH* (dB) |
|---|---|---|---|---|---|---|---|
| | A Milling condition (*Mc*) | B Spindle speed (*n*) | C Feed rate (*f*) | | | | |
| 1 | CM | 3000 | 50 | 0.258 | 11.755 | 95.57 | 39.606 |
| 2 | CM | 3000 | 200 | 0.834 | 1.576 | 99.10 | 39.921 |
| 3 | CM | 3000 | 400 | 2.079 | -6.358 | 112.80 | 41.046 |
| 4 | CM | 5000 | 50 | 0.205 | 13.731 | 81.20 | 38.191 |
| 5 | CM | 5000 | 200 | 0.462 | 6.694 | 88.25 | 38.914 |
| 6 | CM | 5000 | 400 | 1.025 | -0.215 | 101.10 | 40.095 |
| 7 | CM | 7000 | 50 | 0.131 | 17.645 | 80.23 | 38.087 |
| 8 | CM | 7000 | 200 | 0.267 | 11.461 | 86.70 | 38.760 |
| 9 | CM | 7000 | 400 | 0.705 | 3.032 | 96.97 | 39.732 |
| 10 | UAM | 3000 | 50 | 0.257 | 11.777 | 104.40 | 40.374 |
| 11 | UAM | 3000 | 200 | 0.764 | 2.338 | 105.40 | 40.456 |
| 12 | UAM | 3000 | 400 | 1.829 | -5.244 | 115.10 | 41.221 |
| 13 | UAM | 5000 | 50 | 0.249 | 12.049 | 98.93 | 39.906 |
| 14 | UAM | 5000 | 200 | 0.481 | 6.357 | 103.50 | 40.298 |
| 15 | UAM | 5000 | 400 | 0.976 | 0.207 | 106.63 | 40.557 |
| 16 | UAM | 7000 | 50 | 0.169 | 15.402 | 97.90 | 39.815 |
| 17 | UAM | 7000 | 200 | 0.254 | 11.877 | 101.07 | 40.092 |
| 18 | UAM | 7000 | 400 | 0.693 | 3.185 | 103.53 | 40.301 |

### 3.2 Experimental results

The surface roughness and microhardness changes were obtained from the results of the experimental study as shown in Figure 4a and Figure 4b, respectively. Regarding the difference of the milling method, the average of the *Ra* values by the CM method was lower than the UAM at the low feed rate and high spindle speed conditions. However, when increasing the feed rate and decreasing the spindle speed, which is a high chip load per cutting tooth condition, an average of the *Ra* values by UAM trended lower than the CM. For the microhardness results, the UAM displayed an advantage over the CM. This was possibly because the UAM generated workpiece vibration with a high frequency of 19.74 kHz which caused the cutting tool tips to move backward and forward which resulted in an increased temperature at the surface of the workpiece due to the tooltips and workpiece surface and chip contacting loads that led to work-hardening.

In both milling conditions, the surface roughness values exhibited a tendency to decrease with increasing spindle speed. An increase of spindle speed decreased the tool-chip contact area because of the high removal rate of a chip, and this also decreased the time to conduct the friction-providing on the surface. In terms of microhardness, the increase of spindle speed decreases the contact time between the flank face of the cutting tool and workpiece surface, which further weakens the influence of cutting tool on the material work-hardening. In addition, mechanical loads decrease due to a reduction in the shearing stress caused from the increase in spindle speed, thus reducing the potential of plastic deformation of the surface.

The feed rate is the most effective parameter in the increase of surface roughness. As the feed rate increases, it produces thrust forces and vibrations which act on the surface and increase surface roughness. Therefore, an increased feed rate caused a significant increase in the *Ra* values. Similarly, an increase in the feed rate has a substantial effect on the increase of microhardness as a result of high cutting pressure and plastic deformation. Extremely low spindle speeds and high feed rates were observed to be effective in the rise of microhardness caused by the high mechanical load of the machining condition.

As a result, UAM significantly gained an advantage over CM in obtaining high *MH* values. The graphs showing the effects of the control factors obtained with the Taguchi Method (Figure 3a and Figure 3b) on the changes of *Ra* and *MH* verified the results obtained from the experimental studies.

### 3.3. Analysis of variance

Analysis of variance (ANOVA) is a mathematical assessment method to analyze the contribution percentage of each controllable factor in the process response. A larger contribution percentage indicates that the factor is more significant in influencing the performance characteristics. The ANOVA results for the surface roughness and microhardness are shown in Table 6. The analysis used a statistical significance at the confidence level of 95%. The F and percentage value of each control factor were taken into consideration to identify the level of significance of the variables. The percent contributions of the A, B, and C factors on the surface roughness were found to be 0.09%, 23.98%, and 60.86%, respectively (Table 6). Therefore, the most critical factor affecting the surface roughness was feed rate (factor C, 60.86%). According to the ANOVA results, the percent contributions of the A, B, and C factors on microhardness were found to be 31.44%, 25.70%, and 33.23%, respectively. Therefore, the most effective factor on microhardness was feed rate (factor C, 33.23%). The percent error was considered acceptable at 15.08% and 9.63% for *Ra* and *MH*, respectively.

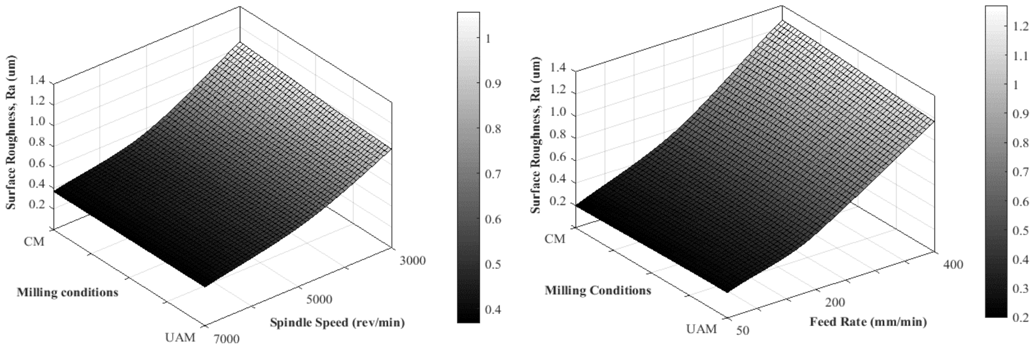


(a)

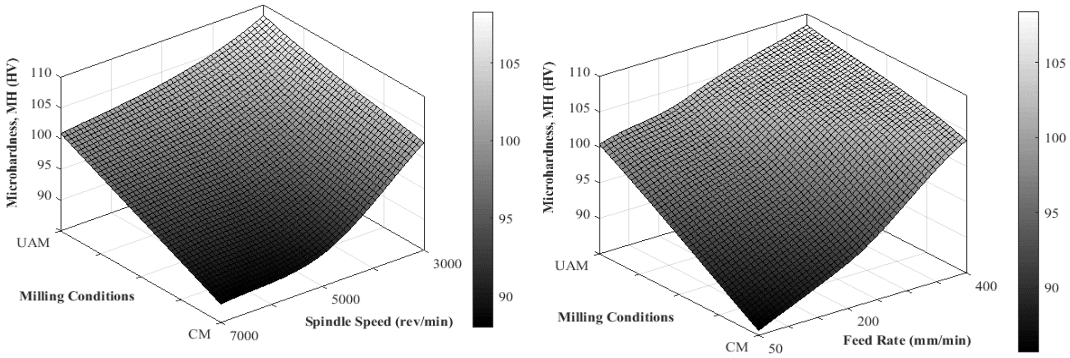


(b)

Figure 4. Effects of the cutting parameters on (a) on surface roughness and (b) microhardness.

Table 6. Results of ANOVA for surface roughness and microhardness.

| Variance source | Degree of freedom (DoF) | Sum of squares (SS) | Mean square (MS) | F ratio | Contribution rate (%) | P value |
|---|---|---|---|---|---|---|
| *Ra* | | | | | | |
| A | 1 | 0.00479 | 0.00479 | 0.07 | 0.09 | 0.792 |
| B | 2 | 1.26197 | 0.63099 | 9.54 | 23.98 | 0.003 |
| C | 2 | 3.20319 | 1.60160 | 24.22 | 60.86 | 0.000 |
| Error | 12 | 0.79347 | 0.06612 | | 15.08 | |
| Total | 17 | 5.26342 | | | 100 | |
| *MH* | | | | | | |
| A | 1 | 496.7 | 496.7 | 39.17 | 31.44 | 0.000 |
| B | 2 | 406.0 | 203.0 | 16.01 | 25.70 | 0.000 |
| C | 2 | 525.0 | 262.5 | 20.70 | 33.23 | 0.000 |
| Error | 12 | 152.2 | 12.68 | | 9.63 | |
| Total | 17 | 1579.8 | | | 100 | |

The predictive equations obtained by the linear regression model of surface roughness and microhardness are defined in Equation 3 and Equation 4.

$$Ra_l = 0.857 - 0.033Mc - 0.000158n + 0.002910f$$
$$(\text{R-square} = 82.50\% \quad \text{R-square Adj} = 78.75\%) \quad (3)$$

$$MH_l = 88.67 + 10.51Mc + 0.002749n + 0.03744f$$
$$\text{R-square} = 87.22\% \quad \text{R-square Adj} = 84.48\% \quad (4)$$

Here $Ra_l$ and $MH_l$ show the predictive equations of surface roughness and microhardness, respectively. Figure 5a shows the comparison of the actual test results and predicted values obtained from the linear regression model. The *R-square* values of the equations obtained from the linear regression model for $Ra_l$ and $MH_l$ were found to be 82.50% and 87.22%, respectively.

The predictive equations for the quadratic regression of surface roughness and microhardness are given in Equation 5 and Equation 6.

$$Ra_q = 0.863 - 0.091Mc - 0.000322n + 0.00557f + 0.000004f^2 + 0.000028Mcn - 0.000377Mcf - 0.000001nf$$
$$(\text{R-square} = 98.70\% \quad \text{R-square Adj} = 96.36\%) \quad (5)$$

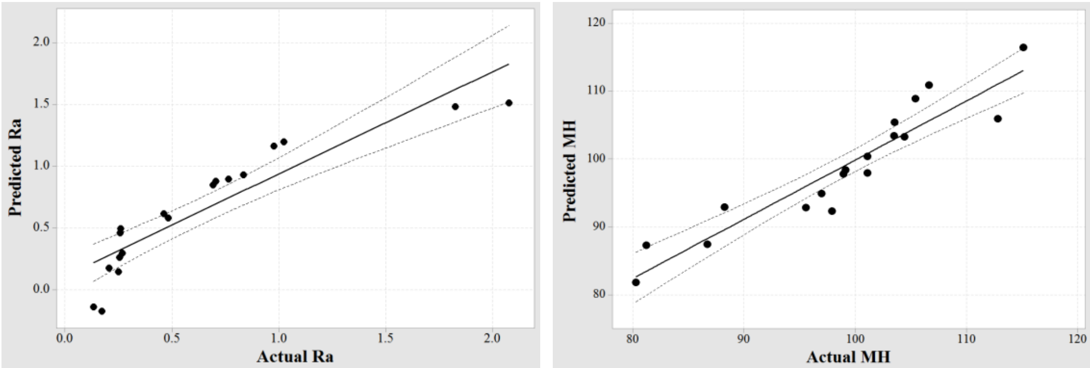


(a)

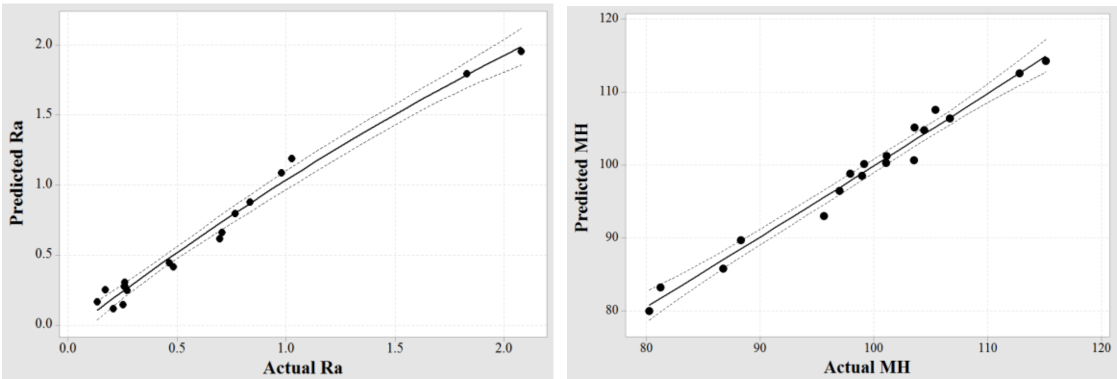


(b)

Figure 5. Comparison of regression model with experimental results for *Ra* and *MH*: (a) linear regression and (b) quadratic regression.

$$MH_q = 109.84 + 7.93Mc - 0.01315n + 0.0725f + 0.000001n^2 + 0.000042f^2 - 0.001764Mcn - 0.02882Mcf + 0.000002nf$$
$$(\text{R-square} = 97.91\% \quad \text{R-square Adj} = 96.05\%) \qquad (6)$$

Here $Ra_q$ and $MH_q$ show the predictive equations for surface roughness and microhardness. Figure 5b shows the test results and the comparison of predicted values which were obtained by the quadratic regression model. The figure tells us that a good relationship exists between the predicted values and test results. The R-square values of the equations obtained by the quadratic regression model for *Ra* and *MH* were found to be 98.70% and 97.91%, respectively. Thus, more intensive predicted values were obtained by the quadratic regression model compared to the linear regression model. As a result, the quadratic regression model was shown to be successful for estimating surface roughness and microhardness.

## 3.5. Estimation of optimum surface roughness and microhardness

Once the optimal level of the design parameters has been selected, the final step is to predict and validate the quality characteristic using the optimal level of the design parameter. The estimated S/N ratio using the optimal level of the design parameters, $\hat{\eta}$ can be calculated as:

$$\hat{\eta} = \eta_m + \sum_{i=1}^{o}(\bar{\eta}_i - \eta_m) \qquad (7)$$

where $\bar{\eta}_i$ is the mean S/N ratio at the optimal level, $\eta_m$ is the total mean S/N ratio, and $o$ is the number of the main design parameters that affect the quality characteristic. The estimated S/N ratio using the optimal cutting parameter for surface roughness and microhardness can be used to estimate the optimum surface roughness and microhardness by Equation 8 and Equation 9, respectively.

$$Ra_{Opt} = 10^{-\hat{\eta}_{Ra}/20} \qquad (8)$$

$$MH_{Opt} = 10^{\hat{\eta}_{MH}/20} \qquad (9)$$

The mean S/N ratio at the optimum level ($\bar{\eta}_i$) for surface roughness and microhardness are represented as (A1, B3, C1) and (A2, B1, C3), respectively, in Table 5. The total mean S/N ratio ($\eta_m$) for surface roughness and microhardness can be calculated from Table 4. As a result of the calculation, it was estimated that $\hat{\eta}_{Ra}$=4.989 dB, $Ra_{Opt}$=0.131 μm, $\hat{\eta}_{MH}$ =41.56 dB, and $MH_{Opt}$=119.69 HV.

### 3.6. Confirmation tests

Confirmation tests for the Taguchi method and re-gression equations at optimum and random levels are shown in Table 7. A comparison of the test results and the predicted values obtained using the Taguchi method (Equations 7–9) and regression equations (Equations 3–6) are given. The predicted values and the experimental values of micro-hardness are close to each other. In terms of surface roughness prediction using the regression equation, the results showed error values higher than the reliable statistical analyses criteria of 20% (Cetin, Ozcelik, Kuram, & Demirbas, 2011). Although the regression model results were not suitable for optimum surface roughness prediction, the Taguchi method still gave a good predicted value. Therefore, the results obtained from the confirmation tests reflected successful optimization except for the surface roughness prediction using the regression equa-tions.

## 4. Conclusions

In this study, the Taguchi method was used to determine the optimal machining parameters in the milling of aluminum A356 with conventional milling and UAM under dry cutting conditions. The experimental results were eva-luated using ANOVA and the following conclusions can be stated.

1. The optimum levels of the control factors for minimizing the surface roughness and maximizing micro-hardness using S/N rates were determined at A1B3C1 (i.e., milling conditions = CM, spindle speed = 7000 rev/min, and feed rate = 50 mm/min) and at A2B1C3 (i.e., milling condi-tions = UAM, spindle speed = 3000 rev/min and feed rate = 400 mm/min), respectively.

2. The statistical analyses revealed that the feed rate was the most significant parameter for surface roughness and microhardness with percent contributions of 60.86% and 33.23%, respectively.

3. CM exhibited slightly better performance than UAM on surface roughness when milling at a low chip load condition, but on the other hand, UAM gave an advantage in surface roughness when cutting at a high chip load condition. The microhardness of UAM was higher than CM in several comparisons. Therefore the recommended milling method and parameter set to use in the milling of aluminum A356 depends on the SI requirement.

4. Quadratic regression models demonstrated a very good relationship with high correlation coefficients (*Ra*=0.963 and *MH*=0.960) between the measured and predicted values for surface roughness and microhardness.

5. According to the confirmation test results, the Taguchi method provided an efficient measured value for the design optimization of the cutting parameters.

In total, the results showed that the Taguchi method was a reliable methodology for parameter optimization on the milling of aluminum A356. The results obtained can be used for academic research as well as for industrial applications. Further studies could consider other factors that affect the SI, such as the depth of cut, cutting tool geometries, vibration frequencies, amplitudes, cutting tool materials, chip breaker, nose radius, and lubricants.

## Acknowledgements

The authors would like to thank Suranaree Uni-versity of Technology and Thammasat University for their support in this research.

## References

Azarhoushang, B., & Akbari, J. (2007). Ultrasonic-assisted drilling of Inconel 738-LC. *International Journal of Machine Tools and Manufacture*, *47*, 1027-1033. doi:10.1016/ j.ijmachtools.2006.10. 007

Chern, GL., & Chang, YC. (2006). Using two-dimensional vibration cutting for micro-milling. *International Journal of Machine Tools and Manufacture*, *46*, 659-666. doi:10.1016/ j.ijmachtools. 2005.07.006

Cetin, N. H., Ozcelik, B., Kuram, E., & Demirbas, E. (2011). Evaluation of vegetable based cutting fluids with extreme pressure and cutting parameters in turning of AISI 304L by Taguchi method. *Journal of Cleaner Production*, *19*, 2049-2056. doi:10.1016/ j.jclepro.2011.07.013

Daymi, A., Boujelbene, M., Amara, B., Bayraktar, E., & Katundi, D. (2011). Surface integrity in high speed end milling of titanium alloy Ti-6Al-4V. *Materials Science and Technology*, *27*(1), 387-394. doi:10. 1179/026708310X12738371692932

Elhami, S., Razfar, M. R., & Farahnakian, M. (2015). Analy-tical, numerical and experimental study of cutting force during thermally enhanced ultrasonic assisted milling of hardened AISI 4140. *International of Mechanical Sciences*, *103*, 158-171. doi:10.1016/j. ijmecsci.2015.09.007

Table 7. Predicted values and confirmation test results by the Taguchi method and regression equations.

| Level | For Taguchi method | | | For linear regression equations | | | For quadratic regression equations | | |
|---|---|---|---|---|---|---|---|---|---|
| | Exp. | Pred. | Error (%) | Exp. | Pred. | Error (%) | Exp. | Pred. | Error (%) |
| *Ra* (µm) | | | | | | | | | |
| A1B3C1 (Optimum) | 0.131 | 0.131 | 0.00 | 0.131 | -0.139 | 205.62 | 0.131 | 0.167 | 27.35 |
| A2B2C2 (Random) | 0.481 | 0.464 | 3.57 | 0.481 | 0.582 | 21.02 | 0.481 | 0.417 | 13.24 |
| *MH* (HV) | | | | | | | | | |
| A2B1C3 (Optimum) | 115.10 | 119.69 | 3.98 | 115.10 | 116.41 | 1.14 | 115.10 | 114.29 | 0.71 |
| A2B1C1 (Random) | 104.40 | 104.73 | 0.31 | 104.40 | 103.31 | 1.04 | 104.40 | 104.78 | 0.36 |

Erkan, O., Demetgul, M., Isik, B., & Tansel, IN. (2014). Selection of optimal machining conditions for the composite materials by using Taguchi and GONNs. *Measurement*, *48*, 306-313. doi:10.1016/j.measurement.2013.11.011

Gupta, A., Singh, H., & Aggarwal, A. (2011). Taguchi-fuzzy multi output optimization (MOO) in high speed CNC turning of AISI P-20 tool steel. *Expert Systems with Applications*, *38*, 6822-6828. doi:10.1016/j.eswa.2010.12.057

Javidi, A., Rieger, U., & Eichlseder, W. (2008). The effect of machining on the surface integrity and fatigue life. *International Journal of Fatigue*, *30*(10-11), 2050-2055. doi:10.1016/j.ijfatigue.2008.01.005

Jin, D., & Liu, Z. (2011). Effect of cutting speed on surface integrity and chip morphology in high-speed machining of PM nickel-based super alloy FGH95. *The International Journal of Advanced Manufacturing Technology*, *60*, 893-899. doi:10.1007/s00170-011-3679-6

Kuram, E., & Ozcelik, B. (2013). Multi-objective optimization using Taguchi based grey relational analysis for micro-milling of Al 7075 material with ball nose end mill. *Measurement*, *46*(6), 1849-1864. doi:10.1016/j.measurement.2013.02.002

Mandal, M., Doloi, B., Mondal, B., & Das, R. (2011). Optimization of flank wear using Zirconia Toughened Alumina (ZTA) cutting tool: Taguchi method and regression analysis. *Measurement*, *44*, 2149-2155. doi:10.1016/j.measurement.2011 .07.022

Maurotto, A., & Wickramarachchi, C.T. (2016). Experimental investigations on effects of frequency in ultrasonically-assisted end-milling of AISI 316L: A feasibility study. *Ultrasonic*c, *65*, 113-120. doi:10.1016/j.ultras.2015.10.012

Noma, K., Takeda, Y., Aoyama, T., Kakinuma, Y., & Hama da, S. (2014). High-precision and high-efficiency micromachining of chemically strengthened glass using ultrasonic vibration. *Procedia CIRP 14*, 389-394. doi:10.1016/j.procir.2014.03.107

Phadke, M. S. (1989). *Quality engineering using robust design*. Englewood Cliffs, NJ: Prentice-Hall.

Rafai, N. H., Lajis, M. A., & Hosni, N. A. J. (2014). The effect of machining parameter on surface integrity when milling hardened steel. *Applied Machanic and Material*, *660*, 70-73. doi:10.4028/www.scientific.net/AMM.660.70

Razfar, M., Sarvi, P. & Zarchi, M. A. (2011). Experimental investigation of the surface roughness in ultrasonic-assisted milling. *Proceedings of the Institution of Mechanical Engineers, Part B: Journal of Engineering Manufacture 225*, 1615-1620. doi:10.1177/0954405411399331

Sayuti, M., Sarhan, A. D., Fadzil, M., & Hamdi, M. (2012). Enhancement and verification of a machined surface quality for glass milling operation-using CBN grinding tool-Taguchi approach. *International Journal of Advanced Manufacturing Technology*, *60*(9-12), 939-950. doi:10.1007/s00170-011-3657-z

Shunyao, Du., Minghe, Chen., Lansheng, Xue., Zhishou, Zhu., & Xinnan, Wang. (2016). Optimization of Process parameter in the high-speed milling of titanium alloy TB17 for surface integrity by the Taguchi-Grey relational analysis method. *Advances in Mechanical Engineering*, *8*(100), 1-12. doi:10.1177/168781401 6671442

Suarez, A., Veiga, F., Luis, L., Polvorosa, R., Steffen, L., & Wretland, A. (2016). Effects of ultrasonic-assisted face milling on surface integrity and fatigue life of Ni-Alloy 718. *Journal of Materials Engineering and Performance*, *25*, 5076-5086. doi:10.1007/s11665-016-2343-6

Sun, J., & Guo, Y.B. (2009). A comprehensive experimental study on surface integrity by end milling Ti-6Al-4V. *Journal of Materials Processing Technology*, *209*, 4036-4042. doi:10.1016/j.jmatprotec.2008.09.022

Uhlmann, E., Protz, F., Stawiszyndski, B. & Heidler, S. (2017). Ultrasonic assisted milling of reinforced plastics. *Procedia CIRP 66*, 164-168. doi:10.1016/j.procir.2017.03.278

Umbrello, D. (2013). Investigation of surface integrity in dry machining of Inconel 718. *The International Journal of Advanced Manufacturing Technology*, *69*, 2183-2190. doi:10.1007/s00170-013-5198-0

Xiangyu, W., Chaunzhen, H., Bin, Z., Guoliang, L., Hongtao, Z., & Jun, W. (2018). Experimental study of surface integrity and fatigue life in the face milling of Inconel 718. *Frontiers of Mechanical Engineering*, *13*(2), 243-250. doi: 10.1007/s11465-018-0479-9